Generalized k-core percolation on correlated and uncorrelated multiplex networks

Yilun Shang
Department of Computer and Information Sciences, Northumbria University, Newcastle upon Tyne, NE1 8ST, UK

It has been recognized that multiplexes and inter-layer degree correlations can play a crucial role in the resilience of many real-world complex systems. Here we introduce a multiplex pruning process that removes nodes of degree less than k_i and their nearest neighbors in layer i for $i = 1, \cdots, m$, and establish a generic framework of generalized **k**-core (G**k**-core) percolation over inter-layer uncorrelated and correlated multiplex networks of m layers, where $\mathbf{k} = (k_1, \cdots, k_m)$ and m is the total number of layers. G**k**-core exhibits a discontinuous phase transition for all **k** owing to cascading failures. We have unraveled the existence of a tipping point of the number of layers, above which the G**k**-core collapses abruptly. This dismantling effect of multiplexity on G**k**-core percolation shows a diminishing marginal utility in homogeneous networks when the number of layers increases. Moreover, we have found the assortative mixing for inter-layer degrees strengthens the G**k**-core but still gives rise to discontinuous phase transitions as compared to the uncorrelated counterparts. Inter-layer disassortativity on the other hand weakens the G**k**-core structure. The impact of correlation effect on G**k**-core tends to be more salient systematically over **k** for heterogenous networks than homogeneous ones.

PACS numbers: 64.60.Ak, 64.60.Fr, 02.10.Ox, 02.50.-r

I. INTRODUCTION

In the last two decades, network science has emerged as a powerful framework to analyze numerous diverse complex systems such as brains, global infrastructures, social networks, and climate systems [1–3]. The resilience (robustness) of such systems is often studied by percolation theory, where the existence of a giant connected component plays a pivotal role in maintaining network structure and functionality when a fraction of nodes and edges are randomly removed from the network [4, 5].

As an important variant of classical percolation mechanism, the k-core percolation [6, 7] progressively removes nodes of degree less than k, i.e. k-leaves, from the network leading to the k-core structure, which is the largest subgraph whose nodes have degree at least k. To quantify the robustness of networks under spreading damage, Azimi-Tafreshi et al. [8] recently proposed a modified leaf pruning algorithm, where k-leaves are recursively removed together with their neighbors and incident edges. The residual network surviving the removal process is referred to as the generalized k-core or Gk-core. The case of $k = 2$ corresponds to the graph-theoretic core notion, which is related to problems of controllability [9], vertex cover and maximum matching [10, 11]. For $k \geq 2$, the Gk-core percolation displays hybrid phase transitions at the critical points of Gk-core in single networks. The attack robustness and stability of Gk-core under various random and intentional attacks have been studied in [12].

Multiplexity, however, has shaken the network percolation theory and gained increasing relevance in the past few years as real-life complex systems are rarely found to be a single network but often an interdependent multilayer structure, where dysfunction of nodes in one layer can lead to failure of dependent nodes in other layers [13–15]. As a result, percolation properties of multiplex networks are drastically different from those of single networks. Multiplex networks, for example, are much more fragile than single networks under random as well as targeted attacks, shifting from continuous to abrupt percolation transitions [13]. The k-core decomposition algorithm has been extended to uncorrelated multiplex networks and intriguing hybrid percolation transitions have been reported in [16, 17].

On top of multiplexity, recent works on classical percolation reveal the profound effect of inter-layer degree correlations [18, 19] and edge overlap [20, 21] in multiplex networks. Such correlations have been observed in many empirical networks. For example, big cities tend to be highly accessible through both highways and airline connections; two friends in social networks are most likely to communicate via both email and cell phone. Albeit of salient relevance, the influence of correlated multiplexity on core based percolation so far has not been adequately understood.

Motivating the above consideration, in this paper we first develop a framework for understanding G**k**-core of uncorrelated multiplex networks with m layers, where $\mathbf{k} = (k_1, k_2, \cdots, k_m)$ and $k_i \geq 2$ for any layer i. By applying a multi-scale pruning algorithm, the G**k**-core can be seen as a natural extension of Gk-core over multiplex networks (see Section II). We find that G**k**-core percolation displays a first-order phase transition for all **k**, and uncover the existence of a tipping point in multiplexes. When the number of layers is above the tipping point, a sudden collapse of G**k**-core occurs. We stress that this phenomenon is not implied by the first-order phase transition of Gk-core percolation. Next, we introduce a correlated multiplex network formalism, which is amenable to analytical treatment of G**k**-core percolation. We show the different effect of correlation in homogeneous (Erdős-Rényi) and heterogenous (log-normal)

multiplex networks. We observe that the assortative mixing of inter-layer degrees tends to build up the $G\mathbf{k}$-core but still gives rise to first-order phase transition for all $\mathbf{k}$. Inter-layer disassortative mixing on the other hand weakens the $G\mathbf{k}$-core structure. Finally, we apply our $G\mathbf{k}$-core percolation algorithms to some real multiplex networks in social interaction, technology and economics.

It is worth noting that our application of pruning process of $G\mathbf{k}$-core to uncorrelated multiplex networks is analogous to [16], where $\mathbf{k}$-core percolation is investigated in uncorrelated multiplex networks. Similarly, the work [17] examined a heterogeneous $\mathbf{k}$-core percolation over interdependent networks with a focus on inter-layer node interdependency. Inter-layer degree distributions, however, are not correlated in these works.

II. ANALYTICAL RESULTS

A. $G\mathbf{k}$-core of uncorrelated multiplex networks

Recall that in multiplex networks, different layers share the same set of nodes [13]. Consider a multiplex network formed by m layers with an arbitrary joint degree distribution $P(\mathbf{q})$ with $\mathbf{q} = (q_1, q_2, \cdots, q_m)$, meaning the probability that a random node has q_i neighbors in layer i for $i = 1, \cdots, m$. Given vector $\mathbf{k} = (k_1, k_2, \cdots, k_m)$, define $\mathbf{k}$-leaf as a node which has intra-layer i degree $q_i < k_i$ for at least one i. We consider the following pruning process: we randomly choose a $\mathbf{k}$-leaf node and delete it together with its neighbors and all incident edges in layer i if $q_i < k_i$. Note that all layers share the same nodes and hence the removal of a node affects all layers and edges incident to it in all layers will be removed accordingly. The process continues until no $\mathbf{k}$-leaves remain in the network. The resulting network is referred to as the $G\mathbf{k}$-core, which is a natural extension of the isolated network version [8, 12]: In the context of disease spreading, a virus is prone to tracking the neighbors of a weak node in each layer. In Fig. 1 we show an example of a duplex network and its $G(2,2)$-core (i.e., $\mathbf{k} = (2,2)$) after the removal process. Note that two components in $\mathbf{k}$ are not symmetric in general unless the two corresponding layers have the same topology and they are uncorrelated.

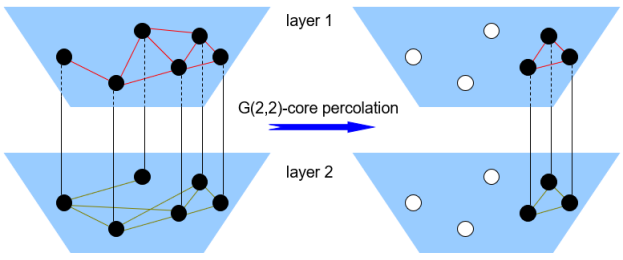

FIG. 1: Schematic illustration of a $G(2,2)$-core percolation on a multiplex network with $m = 2$ layers. White nodes are removed during the cascading removal process.

Our goal is to derive the size of $G\mathbf{k}$-core as a function of the network degree distribution. For $i = 1, \cdots, m$, let $\mathbf{e}_i$ be the i-th unit vector with only the i-th element being one. We divide the nodes into three classes. A node is categorized as α-removable if it is a $(\mathbf{k} - \mathbf{e}_i)$-leaf for at least one i; a node is β-removable if it is a neighbor of a $\mathbf{k}$-leaf node; the rest of the nodes are non-removable and belongs to $G\mathbf{k}$-core. Note that the network has a locally treelike structure as the network size tends to infinity [2]. Given $1 \le i \le m$, denote by α_i, β_i, and $1 - \alpha_i - \beta_i$, respectively, the probabilities that a random neighbor in layer i of a randomly chosen node, say v, is α-removable, β-removable, and non-removable in the network removing node v. Observe that an end node of an edge of layer i extracted at random belongs to the $G\mathbf{k}$-core if it has at least $k_i - 1$ intra-layer i neighbors in the $G\mathbf{k}$-core, at least k_j intra-layer j neighbors in the $G\mathbf{k}$-core for all $j \neq i$, and has no α-removable neighbors. Hence, we derive the self-consistency equation:

$$
\begin{aligned}
&1 - \alpha_i - \beta_i \\
&= \sum_{\mathbf{q} \ge \mathbf{k}} \frac{q_i P(\mathbf{q})}{\langle q_i \rangle} \left[\sum_{s_i = k_i - 1}^{q_i - 1} \binom{q_i - 1}{s_i} (1 - \alpha_i - \beta_i)^{s_i} \beta_i^{q_i - 1 - s_i} \right] \\
&\quad \times \prod_{\substack{j=1 \\ j \neq i}}^{m} \left[\sum_{s_j = k_j}^{q_j} \binom{q_j}{s_j} (1 - \alpha_j - \beta_j)^{s_j} \beta_j^{q_j - s_j} \right], \qquad (1)
\end{aligned}
$$

where $\langle q_i \rangle$ is the average degree of layer i and $\mathbf{q} \ge \mathbf{k}$ means $q_j \ge k_j$ for all $1 \le j \le m$. In (1), $\frac{q_i P(\mathbf{q})}{\langle q_i \rangle}$ represents the probability that the end node of a random edge in layer i has degree $\mathbf{q}$, the combinatorial multiplier $\binom{q_i - 1}{s_i}$ counts the number of ways that one can choose s_i non-removable neighbors among $q_i - 1$ neighbors following intra-layer i edges, and similarly, $\binom{q_j}{s_j}$ counts the choices of s_j non-removable neighbors from q_j neighbors following intra-layer j edges for every $j \neq i$. A random neighbor, say v, in layer i of a random node is β-removable if v has at least one neighbor which is α-removable. Hence,

$$
\beta_i = 1 - \sum_{\mathbf{q} \ge \mathbf{e}_i} \frac{q_i P(\mathbf{q})}{\langle q_i \rangle} (1 - \alpha_i)^{q_i - 1} \prod_{\substack{j=1 \\ j \neq i}}^{m} (1 - \alpha_j)^{q_j}, \qquad (2)
$$

where we recall that $\mathbf{e}_i = (0, \cdots, 0, \overset{i\text{-th}}{1}, 0, \cdots, 0)$ is the i-th unit vector.

Using the expressions (1), (2) and the binomial theorem, we calculate the probability α_i as

$$
\begin{aligned}
\alpha_i = \sum_{\mathbf{q} \ge \mathbf{e}_i} \frac{q_i P(\mathbf{q})}{\langle q_i \rangle} \Bigg\{ & (1 - \alpha_i)^{q_i - 1} \prod_{\substack{j=1 \\ j \neq i}}^{m} (1 - \alpha_j)^{q_j} \\
& - \left[\sum_{s_i = k_i - 1}^{q_i - 1} \binom{q_i - 1}{s_i} (1 - \alpha_i - \beta_i)^{s_i} \beta_i^{q_i - 1 - s_i} \right] \\
& \times \prod_{\substack{j=1 \\ j \neq i}}^{m} \left[\sum_{s_j = k_j}^{q_j} \binom{q_j}{s_j} (1 - \alpha_j - \beta_j)^{s_j} \beta_j^{q_j - s_j} \right] \Bigg\}. \qquad (3)
\end{aligned}
$$

The relative size of the $G\mathbf{k}$-core, denoted by $n_{\mathbf{k}c}$, can be viewed as the probability that a randomly selected node belongs to the $G\mathbf{k}$-core. This event happens if the random node has at least k_i neighbors in layer i for every $1 \leq i \leq m$ according to the pruning process. Hence, we arrive at the expression:

$$n_{\mathbf{k}c} = \sum_{\mathbf{q}\geq\mathbf{k}} P(\mathbf{q}) \times \prod_{i=1}^{m} \Big[\sum_{s_i=k_i}^{q_i} \binom{q_i}{s_i} (1-\alpha_i-\beta_i)^{s_i} \beta_i^{q_i-s_i} \Big]. \quad (4)$$

If we assume that there is no correlation for inter-layer degrees, we write $P(\mathbf{q}) = P_1(q_1)P_2(q_2)\cdots P_m(q_m)$, where $P_i(q_i)$ is the marginal degree distribution in layer i [16]. Define the generating function for the degree of layer i as $G_i(x) = \sum_{q_i=0}^{\infty} P_i(q_i)x^{q_i}$, and its s_i-th derivative as $G_i^{(s_i)}(x) = \sum_{q_i} \frac{q_i!}{(q_i-s_i)!} P_i(q_i)x^{q_i-s_i}$; see e.g. [2]. It follows from (2) and (3) that

$$\begin{aligned}\alpha_i =& \frac{1}{\langle q_i\rangle}\Bigg\{ G_i^{(1)}(1-\alpha_i)\prod_{\substack{j=1\\ j\neq i}}^{m} G_j(1-\alpha_j) \\ &- \Big[G_i^{(1)}(1-\alpha_i) - \sum_{s_i=0}^{k_i-2} \frac{(1-\alpha_i-\beta_i)^{s_i}}{s_i!}\, G_i^{(s_i+1)}(\beta_i)\Big] \\ &\times \prod_{\substack{j=1\\ j\neq i}}^{m} \Big[G_j(1-\alpha_j) \\ &- \sum_{s_j=0}^{k_j-1} \frac{(1-\alpha_j-\beta_j)^{s_j}}{s_j!}\, G_j^{(s_j)}(\beta_j)\Big]\Bigg\} \end{aligned} \quad (5)$$

and

$$\beta_i = 1 - \frac{G_i^{(1)}(1-\alpha_i)}{\langle q_i\rangle} \prod_{\substack{j=1\\ j\neq i}}^{m} G_j(1-\alpha_j). \quad (6)$$

With these expressions, the relative size of the $G\mathbf{k}$-core (4) can be rewritten as

$$\begin{aligned} n_{\mathbf{k}c} =& \prod_{i=1}^{m} \Big[G_i(1-\alpha_i) \\ &- \sum_{s_i=0}^{k_i-1} \frac{(1-\alpha_i-\beta_i)^{s_i}}{s_i!} G_i^{(s_i)}(\beta_i)\Big]. \end{aligned} \quad (7)$$

By solving the self-consistency equations (5), (6) and (7), we can obtain the relative size $n_{\mathbf{k}c}$.

Moreover, the number of layer i edges in the $G\mathbf{k}$-core can be calculated as $(1-\alpha_i-\beta_i)^2 E_i$, where E_i means the total number of edges in layer i. If rescaling this edge number by dividing the total number of nodes, we obtain $(1-\alpha_i-\beta_i)^2 \frac{\langle q_i\rangle}{2}$. Hence, the rescaled number of edges in the $G\mathbf{k}$-core, denoted by $l_{\mathbf{k}c}$, can be calculated as

$$l_{\mathbf{k}c} = \frac{1}{2}\sum_{i=1}^{m} (1-\alpha_i-\beta_i)^2 \langle q_i\rangle. \quad (8)$$

B. $G\mathbf{k}$-core of assortatively correlated multiplex networks

In this section, following the convention of network percolation, we propose a minimalist model of correlated multiplex network by introducing only one additional parameter r. Recall that the joint degree distribution $P(\mathbf{q}) = P(\mathbf{q}; r)$ is the joint probability that a random node has degree q_i in layer i for $1 \leq i \leq m$. Given $1 \leq r \leq m$, the intra-layer degree distributions for layers i ($i = 1, \cdots, r$) are the same, while other layers (if exist) have independent degrees. In other words, the inter-layer degrees are correlated in an assortative mixing manner [22]. Let $\delta_{a,b}$ be the Kronecker's delta function. The joint degree distribution of the correlated multiplex network model is described by

$$\begin{aligned} P(\mathbf{q}; r) =& P_1(q_1)\delta_{q_2,q_1}\cdots\delta_{q_r,q_1}P_{r+1}(q_{r+1})\cdots P_m(q_m). \end{aligned} \quad (9)$$

Clearly, the case of $r = 1$ reduces to the uncorrelated multiplex network model discussed in Section II.A. Furthermore, with the degree distribution (9), the expressions (1)-(4) still apply.

To solve the relative size $n_{\mathbf{k}c}$ of the $G\mathbf{k}$-core, we introduce a version of high dimensional generating function as

$$\begin{aligned} &G(x_1, x_2, \cdots, x_m) \\ &= \sum_{q_1=0}^{\infty} \sum_{\substack{q_j=0\\ j=r+1,\cdots,m}}^{\infty} P_1(q_1)P_{r+1}(q_{r+1})\cdots P_m(q_m) \\ &\quad \times (x_1x_2\cdots x_r)^{q_1} \cdot x_{r+1}^{q_{r+1}}\cdots x_m^{q_m}, \end{aligned} \quad (10)$$

which is a generalization of single variable generating functions [19, 23, 24] and some other versions have already been studied in the study of, e.g., network percolation with community structure [5]. By using (2), (3) and some algebra, we can derive in a similar manner as

in (5):

$$\begin{aligned}\alpha_i =&\frac{1}{\langle q_i\rangle}\Bigg\{\sum_{\substack{s_j=0\\ j\neq i,j=1,\cdots,m}}^{k_j-1}\frac{(1-\alpha_j-\beta_j)^{s_j}}{s_j!}\\ &\times G^{(s_1,\cdots,s_{j-1},1,s_{j+1},\cdots,s_m)}(\beta_1,\cdots,\beta_{j-1},1-\alpha_j,\\ &\beta_{j+1},\cdots,\beta_m)\\ &+\sum_{s_i=0}^{k_i-2}\frac{(1-\alpha_i-\beta_i)^{s_i}}{s_i!}G^{(0,\cdots,0,\overset{i\text{-th}}{s_i+1},0,\cdots,0)}(1-\alpha_1,\\ &\cdots,1-\alpha_{i-1},\beta_i,1-\alpha_{i+1},\cdots,1-\alpha_m)\\ &-\sum_{s_i=0}^{k_i-2}\sum_{\substack{s_j=0\\ j\neq i,j=1,\cdots,m}}^{k_j-1}\frac{(1-\alpha_i-\beta_i)^{s_i}}{s_i!}\\ &\times\prod_{\substack{j=1\\ j\neq i}}^{m}\frac{(1-\alpha_j-\beta_j)^{s_j}}{s_j!}\\ &\times G^{(s_1,\cdots,s_{i-1},s_i+1,s_{i+1},\cdots,s_m)}(\beta_1,\cdots,\beta_m)\Bigg\}\end{aligned}\tag{11}$$

and

$$\beta_i=1-\frac{G^{(0,\cdots,0,\overset{i\text{-th}}{1},0,\cdots,0)}(1-\alpha_1,\cdots,1-\alpha_m)}{\langle q_i\rangle},\tag{12}$$

where (in the light of (10))

$$\begin{aligned}&G^{(s_1,\cdots,s_m)}(x_1,\cdots,x_m)\\ =&\Big[\sum_{q_1=0}^{\infty}(q_1!)^r P_1(q_1)\prod_{j=1}^{r}\frac{x_j^{q_1-s_j}}{(q_1-s_j)!}\Big]\\ &\times\prod_{j=r+1}^{m}\Big[\sum_{q_j=0}^{\infty}\frac{q_j!P_j(q_j)}{(q_j-s_j)!}x_j^{q_j-s_j}\Big],\end{aligned}\tag{13}$$

describes the mixed $(s_1,\cdots,s_m)$ partial derivative of the generating function. As the inter-layer degrees are correlated, the fiddly application of mixed derivatives above is essential.

In view of (4) and (13), the relative size of the $G\mathbf{k}$-core becomes

$$\begin{aligned}n_{\mathbf{k}c}=&G(1-\alpha_1,\cdots,1-\alpha_m)\\ &-\sum_{\substack{s_i=0\\ i=1,\cdots,m}}^{k_i-1}\Big[\prod_{i=1}^{m}\frac{(1-\alpha_i-\beta_i)^{s_i}}{s_i!}\Big]\\ &\cdot G^{(s_1,\cdots,s_m)}(\beta_1,\cdots,\beta_m).\end{aligned}\tag{14}$$

The rescaled number of edges in the $G\mathbf{k}$-core can be derived in a similar manner as in (8).

C. $G\mathbf{k}$-core of disassortatively correlated multiplex networks

In a disassortatively correlated multiplex network, a node of certain degree tends to connect to a node in another layer with dissimilar degree. Some different mechanisms of disassortative correlation have been studied in the literature, e.g. [25–28]. By convention, we consider a duplex network with $m=2$ and we here adopt a philosophy akin to Section II.B by specifying the joint degree distribution as

$$P(\mathbf{q})=P_1(q_1)\delta_{q_2,\Delta-q_1},\tag{15}$$

where Δ is the maximum degree of the layer 1 network. We define the associated generating function as

$$H(x_1,x_2)=\sum_{q_1=0}^{\Delta}P_1(q_1)x_1^{q_1}x_2^{\Delta-q_1}.\tag{16}$$

For $i=1,2$, it can be shown that the parameters α_i, β_i, $n_{\mathbf{k}c}$, and $l_{\mathbf{k}c}$ are given by (11), (12), (14), and (8) respectively, with $m=2$ and G replaced by H.

III. SYNTHETIC NETWORKS

In this section, we perform numerical simulations for some benchmark models with Erdős-Rényi (ER) multiplex networks and heavy tailed log-normal multiplex networks. In the simulations, networks have node size $N=10^7$ to 5×10^7 to approximate the thermodynamic limit. Note that scale-free networks only have trivial cores even for a single layer [10].

A. Multiplex Erdős-Rényi networks

1. *Uncorrelated layers*

We first consider the uncorrelated duplex ER networks with $m=2$ and marginal Poisson degree distributions. The combined degree distribution is given by $P(\mathbf{q})=P_1(q_1)P_2(q_2)=e^{-(\lambda_1+\lambda_2)}\frac{\lambda_1^{q_1}\lambda_2^{q_2}}{q_1!q_2!}$ for $q_1,q_2\geq0$, where λ_i is the average degree of layer i for $i=1,2$. For simplicity, we assume the symmetric case with $\lambda:=\lambda_1=\lambda_2$ and hence $G_1(x)=G_2(x)=e^{\lambda(x-1)}$.

Fig. 2 shows the relative size $n_{\mathbf{k}c}$ and the rescaled number of edges $l_{\mathbf{k}c}$ of the $G\mathbf{k}$-core in duplex ER networks as well as their counterparts in single ER networks. The simulations agree well with the theoretical predictions in all cases. We observe that for all degrees $\mathbf{k}$, the $G\mathbf{k}$-core percolation displays a discontinuous phase transition in duplex ER networks. This differs from single network scenarios, where $G2$-core has a continuous percolation transition while Gk-core ($k\geq3$) has first-order transitions. The catastrophic failure of $G\mathbf{k}$-core caused by interdependent multiplex structure echoes those previously discovered for k-core percolation [16, 17] as well as classical ones [13, 29].

As one would expect, the rescaled number of edges in the $G\mathbf{k}$-core of duplex networks asymptotically doubles that in the single networks as the ER network becomes

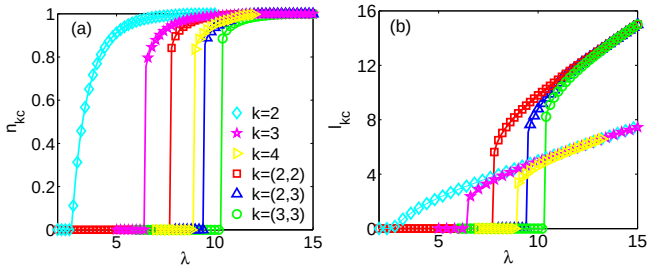

FIG. 2: The relative fraction $n_{\mathbf{k}c}$ of $G\mathbf{k}$-core and rescaled number of edges $l_{\mathbf{k}c}$ of $G\mathbf{k}$-core in single and uncorrelated duplex ER networks for $k = 2$ (cyan diamonds), $k = 3$ (magenta stars), $k = 4$ (yellow right triangles), $\mathbf{k} = (2, 2)$ (red squares), $\mathbf{k} = (2, 3)$ (blue upper triangles), $\mathbf{k} = (3, 3)$ (green circles). The lines are theoretical results and data points are based on simulations averaged over 40 realizations of networks with 10^7 nodes and mean degree λ.

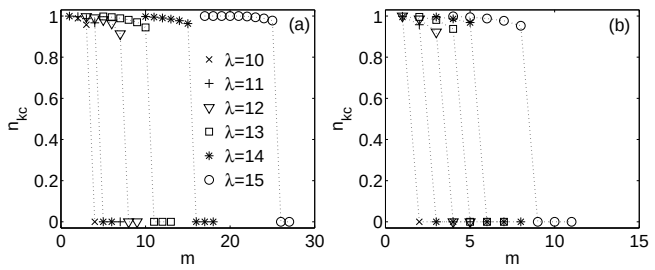

FIG. 3: The relative fraction $n_{\mathbf{k}c}$ of $G\mathbf{k}$-core as a function of layer number m in uncorrelated multiplex ER networks with different mean degree: $\lambda = 10$ (crosses), $\lambda = 11$ (pluses), $\lambda = 12$ (lower triangles), $\lambda = 13$ (squares), $\lambda = 14$ (asterisks), $\lambda = 15$ (circles) for (a) $\mathbf{k} = (2, 2, \cdots, 2)$ and (b) $\mathbf{k} = (3, 3, \cdots, 3)$. The lines are theoretical results and data points are based on simulations averaged over 30 realizations of networks with 10^7 nodes.

dense (i.e., when λ grows); see Fig. 2(b). When comparing Fig. 2(a) with Fig. 2(b), it can be seen that the critical values of connectivity λ coincide for $n_{\mathbf{k}c}$ and the corresponding $l_{\mathbf{k}c}$.

The influence of multiplex architecture can be better appreciated in Fig. 3, where $n_{\mathbf{k}c}$ is plotted as a function for a range of m, the number of layers. A couple of interesting observations are in order. Firstly, the tipping point, where the $G\mathbf{k}$-core is suddenly fragmented, can be identified for ER networks with any given λ. For example, the tipping point of $G(2, 2, \cdots, 2)$-core percolation for ER networks having $\lambda = 10$ is $m = 4$ (see Fig. 3(a)), and that of $G(3, 3, \cdots, 3)$-core percolation is $m = 2$ (see Fig. 3(b)). Notice that this dramatic drop of $n_{\mathbf{k}c}$ with respect to m is not implied by the first-order percolation for a given multiplex network (with fixed m) as observed in Fig. 2. Secondly, although the more layers the more fragile the network becomes, the effect of multiplexity on $G\mathbf{k}$-core tends to decrease as m grows — a multiplex network version of 'diminishing marginal utility'. This phenomenon is demonstrated by the increasing gaps between lines in Fig. 3 when m increases steadily.

2. *Correlated layers*

We next consider the correlated duplex ER networks with $r = m = 2$. For the assortatively correlated network, the network has degree distribution $P(\mathbf{q}) = P_1(q_1)\delta_{q_2,q_1}$ with Poisson distribution $P_1(q_1) = e^{-\lambda}\frac{\lambda^{q_1}}{q_1!}$. The joint generating function is given by $G(x_1, x_2) = e^{\lambda(x_1x_2-1)}$.

In Fig. 4, we show the relative size $n_{\mathbf{k}c}$ and the rescaled number of edges $l_{\mathbf{k}c}$ of the $G\mathbf{k}$-core in both assortatively correlated and uncorrelated duplex ER networks. The simulations are consistent with the theoretical predictions in Section II.B. For all degrees $\mathbf{k}$, the $G\mathbf{k}$-cores display discontinuous transitions in both uncor-

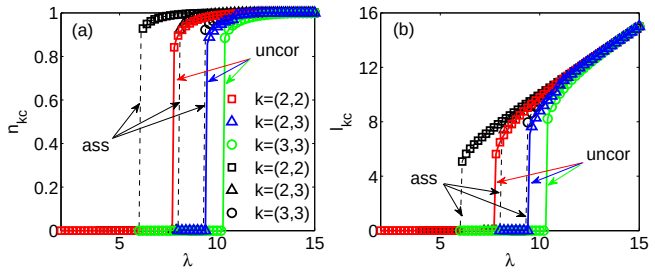

FIG. 4: The relative fraction $n_{\mathbf{k}c}$ of $G\mathbf{k}$-core and rescaled number of edges $l_{\mathbf{k}c}$ of $G\mathbf{k}$-core in uncorrelated duplex ER networks for $\mathbf{k} = (2, 2)$ (red squares), $\mathbf{k} = (2, 3)$ (blue triangles), $\mathbf{k} = (3, 3)$ (green circles) and assortatively correlated duplex ER networks for $\mathbf{k} = (2, 2)$ (black squares), $\mathbf{k} = (2, 3)$ (black triangles), $\mathbf{k} = (3, 3)$ (black circles). The lines are theoretical results and data points are based on simulations averaged over 40 realizations of networks with 10^7 nodes and mean degree λ.

related and correlated networks. Moreover, compared to uncorrelated counterparts, assortatively correlated networks have larger $G\mathbf{k}$-cores. This phenomenon can be attributed to the lower possibility of cascading failure due to the stringent inter-layer degree correlation. Also, comparing Fig. 4(a) with Fig. 4(b), we observe hat the critical values of connectivity λ coincide for $n_{\mathbf{k}c}$ and the corresponding $l_{\mathbf{k}c}$.

For the disassortatively correlated network, the network has degree distribution $P(\mathbf{q}) = P_1(q_1)\delta_{q_2,\Delta-q_1}$ with Poisson distribution $P_1(q_1) = e^{-\lambda}\frac{\lambda^{q_1}}{q_1!}$ and $\Delta = (\ln\ln N)^{-1}\ln N$ [30]. Note that in the disassortatively correlated model, only the layer 1 follows strictly the ER network degree distribution. In Fig. 5 we compare the relative size $n_{\mathbf{k}c}$ and the rescaled number of edges $l_{\mathbf{k}c}$ of the $G\mathbf{k}$-core in both correlated and uncorrelated duplex ER networks. We similarly observed discontinuous phase transition at critical values of λ for all degrees $\mathbf{k}$ as in Fig. 4. However, the disassortativity tends to weaken

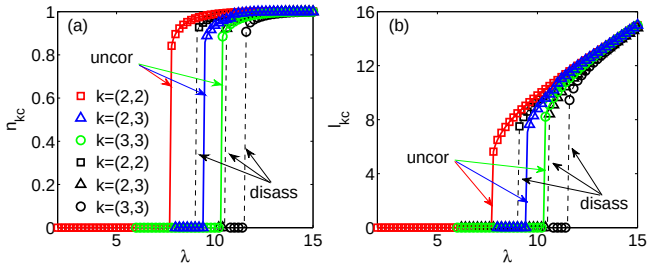

FIG. 5: The relative fraction $n_{\mathbf{k}c}$ of $G\mathbf{k}$-core and rescaled number of edges $l_{\mathbf{k}c}$ of $G\mathbf{k}$-core in uncorrelated duplex ER networks for $\mathbf{k} = (2, 2)$ (red squares), $\mathbf{k} = (2, 3)$ (blue triangles), $\mathbf{k} = (3, 3)$ (green circles) and disassortatively correlated duplex ER networks for $\mathbf{k} = (2, 2)$ (black squares), $\mathbf{k} = (2, 3)$ (black triangles), $\mathbf{k} = (3, 3)$ (black circles). The lines are theoretical results and data points are based on simulations averaged over 40 realizations of networks with 10^7 nodes and mean degree λ.

the $G\mathbf{k}$-core in all cases, which is in sharp contrast to assortatively correlated ones as one would expect.

B. Multiplex log-normal networks

1. *Uncorrelated layers*

As a second example, we consider the uncorrelated duplex networks with $m = 2$ and asymptotic log-normal degree distribution $P(\mathbf{q}) = P_1(q_1)P_2(q_2) \propto \exp\big(-\frac{(\ln q_1-\sigma_1)^2+(\ln q_2-\sigma_2)^2}{4}\big)$ for $q_1, q_2 \geq 1$. The log-normal distribution $P_1(q_1)$ is heavy tailed and skewed with mode e^{σ_1-2} and mean e^{σ_1+1}. Some growing networks such as citation networks are found to have log-normal degree distributions [31, 32]. For simplicity, we assume the symmetric case with $\sigma := \sigma_1 = \sigma_2 \in (-\infty, \infty)$.

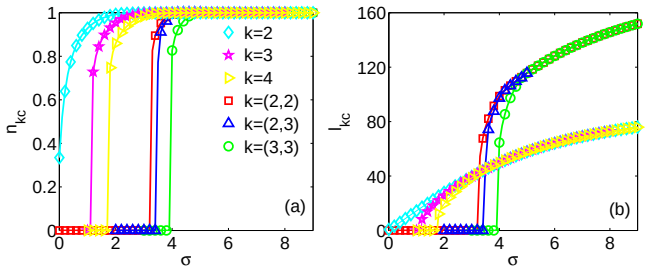

FIG. 6: The relative fraction $n_{\mathbf{k}c}$ of $G\mathbf{k}$-core and rescaled number of edges $l_{\mathbf{k}c}$ of $G\mathbf{k}$-core in single and uncorrelated duplex log-normal networks for $k = 2$ (cyan diamonds), $k = 3$ (magenta stars), $k = 4$ (yellow right triangles), $\mathbf{k} = (2, 2)$ (red squares), $\mathbf{k} = (2, 3)$ (blue upper triangles), $\mathbf{k} = (3, 3)$ (green circles). The lines are theoretical results and data points are based on simulations averaged over 40 realizations of networks with 5×10^7 nodes and parameter σ.

The relative size $n_{\mathbf{k}c}$ and the rescaled number of edges $l_{\mathbf{k}c}$ of the $G\mathbf{k}$-core in duplex log-normal networks as well as their counterparts in single layer log-normal networks are show in Fig. 6. Similarly as in the ER case, the $G\mathbf{k}$-core percolation displays a discontinuous phase transition for all degrees $\mathbf{k}$, and Gk-core percolation for $(k \geq 3)$ has discontinuous phase transitions. It is worth noting that multiplexity causes much more harm to the structural resilience to log-normal networks than ER networks. For example, $G(2, 2)$-core is larger than $G4$-core for ER networks in Fig. 2 while $G(2, 2)$-core becomes much smaller than $G4$-core for log-normal networks in Fig. 6. This discrepancy can be explained by the heterogenous degree distribution of the log-normal network, where low-degree nodes are likely connected to hubs spreading the pruning process farther.

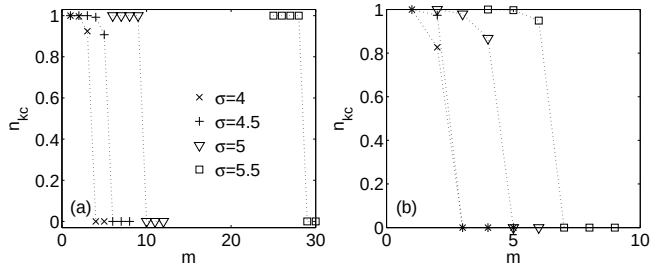

FIG. 7: The relative fraction $n_{\mathbf{k}c}$ of $G\mathbf{k}$-core as a function of layer number m in uncorrelated multiplex log-normal networks with different parameter σ: $\sigma = 4$ (crosses), $\sigma = 4.5$ (pluses), $\sigma = 5$ (triangles), $\sigma = 5.5$ (squares) for (a) $\mathbf{k} = (2, 2, \cdots, 2)$ and (b) $\mathbf{k} = (3, 3, \cdots, 3)$. The lines are theoretical results and data points are based on simulations averaged over 30 realizations of networks with 5×10^7 nodes.

In Fig. 7, we display $n_{\mathbf{k}c}$ as a function of the number of layers m. Like in the ER cases above, we observe the tipping points for $G\mathbf{k}$-core percolation in log-normal multiplex networks. For instance, when $\sigma = 4$, the tipping point of $G(2, 2, \cdots, 2)$-core percolation for log-normal networks is $m = 4$ (see Fig. 7(a)) — which is the critical point where $n_{\mathbf{k}c}$ drops to zero abruptly. The tipping point of $G(3, 3, \cdots, 3)$-core for the same network reduces to $m = 3$ as one would expect (see Fig. 7(b)).

Note that the density of log-normal network is expressed in an exponential function of σ, roughly proportional to e^{σ}. This means the span of density is unequal, for example, from $\sigma = 4$ to $\sigma = 4.5$ and to $\sigma = 5$ (see Fig. 7). Hence, the effect of multiplexity ('diminishing marginal utility') on $G\mathbf{k}$-core is less obvious compared to the ER cases in Fig. 3.

2. *Correlated layers*

We next consider the assortatively correlated duplex log-normal networks with $r = m = 2$. The network has degree distribution $P(\mathbf{q}) = P_1(q_1)\delta_{q_2,q_1}$ with log-normal distribution $P_1(q_1) \propto \exp\big(-\frac{(\ln q_1-\sigma)^2}{4}\big)$.

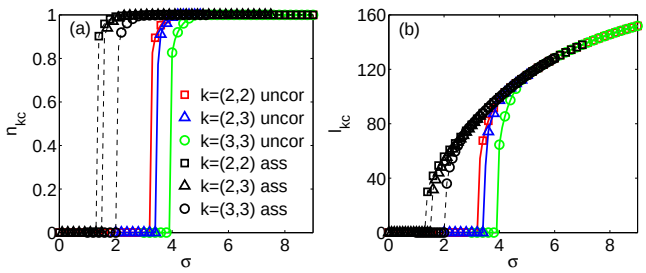

FIG. 8: The relative fraction $n_{\mathbf{k}c}$ of $G\mathbf{k}$-core and rescaled number of edges $l_{\mathbf{k}c}$ of $G\mathbf{k}$-core in uncorrelated duplex log-normal networks for $\mathbf{k} = (2,2)$ (red squares), $\mathbf{k} = (2,3)$ (blue triangles), $\mathbf{k} = (3,3)$ (green circles) and assortatively correlated duplex log-normal networks for $\mathbf{k} = (2,2)$ (black squares), $\mathbf{k} = (2,3)$ (black triangles), $\mathbf{k} = (3,3)$ (black circles). The lines are theoretical results and data points are based on simulations averaged over 40 realizations of networks with 5×10^7 nodes and parameter σ.

We compare in Fig. 8 the relative size $n_{\mathbf{k}c}$ and the rescaled number of edges $l_{\mathbf{k}c}$ of the $G\mathbf{k}$-core in assortatively correlated duplex log-normal with uncorrelated ones. It is found that for all degrees $\mathbf{k}$, the $G\mathbf{k}$-cores show discontinuous transitions in both uncorrelated and correlated scenarios. Moreover, similarly as in ER cases, the correlation between two layers suppresses the damage of cascading failure as is demonstrated by larger $G\mathbf{k}$-cores in the correlated networks. Due to the heterogeneity of intra-layer degree distribution, this mitigation effect is even more apparent as compared to Fig. 4. For example, in Fig. 8 $G(3,3)$-core in a assortatively correlated network is considerably larger than $G(2,2)$-core in an uncorrelated network. In Fig. 4, however, this relation is seen to be inverted.

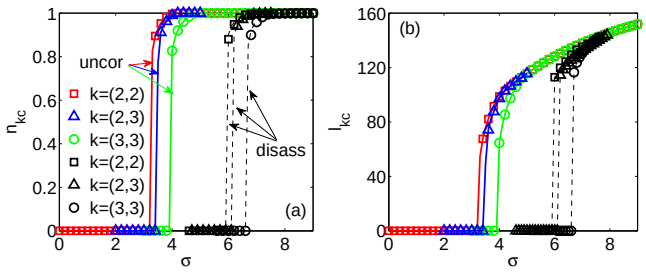

FIG. 9: The relative fraction $n_{\mathbf{k}c}$ of $G\mathbf{k}$-core and rescaled number of edges $l_{\mathbf{k}c}$ of $G\mathbf{k}$-core in uncorrelated duplex log-normal networks for $\mathbf{k} = (2,2)$ (red squares), $\mathbf{k} = (2,3)$ (blue triangles), $\mathbf{k} = (3,3)$ (green circles) and disassortatively correlated duplex log-normal networks for $\mathbf{k} = (2,2)$ (black squares), $\mathbf{k} = (2,3)$ (black triangles), $\mathbf{k} = (3,3)$ (black circles). The lines are theoretical results and data points are based on simulations averaged over 40 realizations of networks with 5×10^7 nodes and parameter σ.

For the disassortatively correlated network, it has degree distribution $P(\mathbf{q}) = P_1(q_1)\delta_{q_2,\Delta-q_1}$ with log-normal distribution $P_1(q_1) \propto \exp\big(-\frac{(\ln q_1 - \sigma)^2}{4}\big)$ and $\Delta = N-1$ [33]. In this model, both layer 1 and layer 2 are skewed, having heterogeneous degree distributions. In Fig. 9 we compare the relative size $n_{\mathbf{k}c}$ and the rescaled number of edges $l_{\mathbf{k}c}$ of the $G\mathbf{k}$-core in both disassortatively correlated and uncorrelated duplex log-normal networks. Similarly as in Fig. 8, we observed discontinuous phase transition at critical values of σ for all degrees $\mathbf{k}$. As in the ER network situation, the disassortativity here again significantly weaken the $G\mathbf{k}$-core in all cases as compared to uncorrelated layers.

IV. REAL MULTIPLEX NETWORKS

We consider some real-life multiplex networks with characteristics summarized in Table 1 and apply the computational framework of $G\mathbf{k}$-core percolation over these networks. The first one is a guarantee market network with nodes representing companies and edges joint liability guarantee relationships in China's guarantee circle [34]. Both layer 1 (for the year 2013) and layer 2 (for the year 2014) follow scale-free degree distributions and they are assortatively correlated with the Pearson's coefficient 0.33. The second example is a friendship network extracted from online social media BlogCatalog (layer 1) and Flickr (layer 2), where nodes are users and edges are friendship connections [35]. Both layers have scale-free structures. The third network comes from Internet topology at the autonomous system level with layer 1 representing IPv4 relationship and layer 2 IPv6 relationship over autonomous system nodes [36].

In Fig. 10 we show the relative size of $G\mathbf{k}$-cores in these multiplex networks for different $\mathbf{k}$ against their theoretical results based on our multiplex network models, where the degree distribution of the empirical networks are fed in. It can be seen that the predictions based on uncorrelated and assortatively correlated models are more accurate than that using disassortatively correlated models generally. This phenomenon is in line with the positive Pearson coefficients for all these networks; c.f. Table 1. On can see from Fig. 10 that, in some cases, there are noticeable discrepancies between theory and reality. Arguably, the inner layer structure such as intra-layer correlation, motif and clustering also influence the $G\mathbf{k}$-cores in real world large-scale networks [8, 12].

V. CONCLUSION

In this paper a pruning process is introduced to produce generalized $\mathbf{k}$-core, i.e. $G\mathbf{k}$-core, in the context of multiplex networks. We have presented a general analytical framework for investigating $G\mathbf{k}$-core percolation over uncorrelated and correlated multiplex networks. It is shown that $G\mathbf{k}$-core has a discontinuous phase transition for all degree $\mathbf{k}$, different from Gk-core in single networks [8, 12]. We have revealed the existence of a tipping

	N	E_1	E_2	Δ_1	Δ_2	$d_{\rm ave}$	ρ
Market [34]	4354	3618	4102	83	91	1.77	0.33
Friendship [35]	10312	333983	574802	3992	4898	88.13	0.09
Internet [36]	4819	11601	12045	306	339	4.90	0.24

TABLE I: List of three empirical multiplex networks analyzed in this paper. N: number of nodes; E_i: number of edges in layer i; Δ_i: maximum degree in layer i; $d_{\rm ave}$: average degree; ρ: Pearson's correlation coefficient.

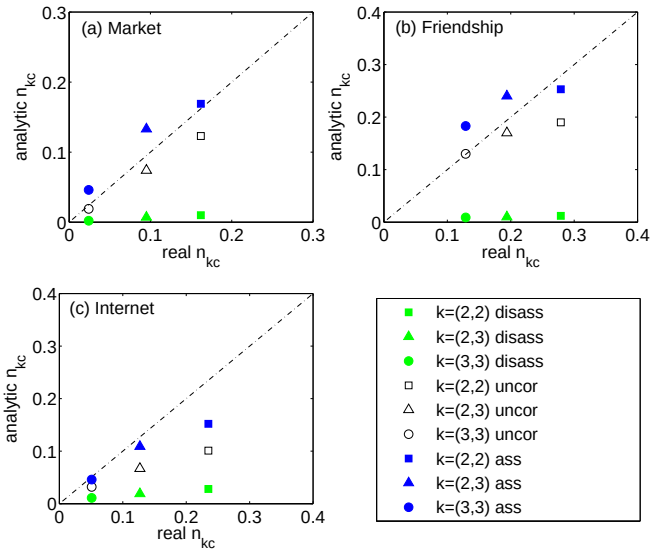

FIG. 10: The relative fraction $n_{\mathbf{k}c}$ of $G\mathbf{k}$-core in (a) Market network, (b) Friendship network, and (c) Internet versus theoretical predictions via uncorrelated and correlated multiplex networks for $\mathbf{k} = (2, 2)$ (squares), $\mathbf{k} = (2, 3)$ (triangles), and $\mathbf{k} = (3, 3)$ (circles). In assortatively and disassortatively correlated models, layer 1 follows empirical distributions.

point of the number of layers, over which the $G\mathbf{k}$-core dismantles abruptly. Interestingly, the depreciating effect of multiplexity on $G\mathbf{k}$-core percolation in multiplex ER networks shows an evident diminishing marginal utility. This implies that dense homogeneous multiplex networks are potentially able to sustain more layers under $G\mathbf{k}$-core percolation than one might expect. We found that the assortative mixing in inter-layer degrees strengthens the $G\mathbf{k}$-core but still leads to discontinuous phase transition as compared to the uncorrelated counterparts. Disassortative mixing, on the contrary, gives rise to weaker $G\mathbf{k}$-core for all $\mathbf{k}$. These inter-layer degree correlation induced effects tend to be more salient systematically in heterogenous networks than homogeneous ones.

The depreciation caused by multiplexity in terms of $G\mathbf{k}$-core in uncorrelated multiplex networks discovered here is qualitatively similar to the observation for k-core in [16, 17]. The removal of nearest neighbors of weak nodes $G\mathbf{k}$-core percolation characterizes a specific robustness under spreading damage. Studying the mixing of inter-layer degree distributions enhances our understanding on the impact of multiplexity and correlation on robustness in real world systems, where subsequent damage or contact infection is likely in the neighborhood of a compromised node. The results will enable use to design robust complex systems and optimize structural correlation in response to virus-like attacks.

Acknowledgment

The author would like to thank the reviewers for their detailed valuable comments that improved the quality of the paper. This work was supported in part by UoA Flexible Fund (Grant No. 201920A1001) and Northumbria University.

[1] D. J. Watts and S. H. Strogatz, Nature **393**, 440 (1998).
[2] M. E. J. Newman, *Networks, 2nd Edition* (Oxford University Press, Oxford, 2018).
[3] N. Boers, B. Goswami, A. Rheinwalt, B. Bookhagen, B. Hoskins, and J. Kurths, Nature **566**, 373 (2019).
[4] R. Cohen and S. Havlin, *Complex Networks: Structure, Robustness and Function* (Cambridge University Press, Cambridge, 2010).
[5] G. Dong, J. Fan, L. M. Shekhtman, S. Shai, R. Du, L. Tian, X. Chen, H. E. Stanley, and S. Havlin, Proc. Natl. Acad. Sci. U.S.A **115**, 6911 (2018).
[6] S. N. Dorogovtsev, A. V. Goltsev, and J. F. F. Mendes, Phys. Rev. Lett. **96**, 040601 (2006).
[7] G. J. Baxter, S. N. Dorogovtsev, K.-E. Lee, J. F. F. Mendes, and A. V. Goltsev, Phys. Rev. X **5**, 031017 (2015).
[8] N. Azimi-Tafreshi, S. Osat, and S. N. Dorogovtsev, Phys. Rev. E **99**, 022312 (2019).
[9] Y.-Y. Liu, J.-J. Slotine, and A.-L. Barabási, Nature **473**, 167 (2011).
[10] Y.-Y. Liu, E. Csóka, H. Zhou, and M. Pósfai, Phys. Rev. Lett. **109**, 205703 (2012).
[11] C. Witt, Theor. Comput. Sci. **425**, 117 (2012).
[12] Y. Shang, New J. Phys. **21**, 093013 (2019).
[13] S. Boccaletti, G. Bianconi, R. Criado, C. I. del Genio, J. Gómez-Gardeñes, M. Romance, I. Sendiña-Nadal, Z. Wang, and M. Zanin, Phys. Rep. **544**, 1 (2014).
[14] F. Radicchi and G. Bianconi, Phys. Rev. X **7**, 011013 (2017).
[15] M. M. Danziger, I. Bonamassa, S. Boccaletti, and

S. Havlin, Nat. Phys. **15**, 178 (2019).
[16] N. Azimi-Tafreshi, J. Gómez-Gardeñes, and S. N. Dorogovtsev, Phys. Rev. E **90**, 032816 (2014).
[17] N. K. Panduranga, J. Gao, X. Yuan, H. E. Stanley, and S. Havlin, Phys. Rev. E **96**, 032317 (2017).
[18] B. Min, S. D. Yi, K.-M. Lee, and K.-I. Goh, Phys. Rev. E **89**, 042811 (2014).
[19] A. Hackett, D. Cellai, S. Gómez, A. Arenas, and J. P. Gleeson, Phys. Rev. E **6**, 021002 (2016).
[20] D. Cellai, S. N. Dorogovtsev, and G. Bianconi, Phys. Rev. E **94**, 032301 (2016).
[21] S. Osat, A. Faqeeh, and F. Radicchi, Nat. Commun. **8**, 1540 (2017).
[22] M. E. J. Newman, Phys. Rev. Lett. **89**, 208701 (2002).
[23] M. E. J. Newman, S. H. Strogatz, and D. J. Watts, Phys. Rev. E **64**, 026118 (2001).
[24] Y. Shang, Phys. Rev. E **90**, 032820 (2014).
[25] R. Parshani, C. Rozenblat, D. Ietri, C. Ducruet, and S. Havlin, EPL **92**, 68002 (2011).
[26] V. Nicosia, G. Bianconi, V. Latora, and M. Barthelemy, Phys. Rev. Lett. **111**, 058701 (2013).
[27] V. Nicosia and V. Latora, Phys. Rev. E **92**, 032805 (2015).
[28] K.-M. Lee, J. Y. Kim, W.-K. Cho, K.-I. Goh, and I.-M. Kim, New J. Phys. **14**, 033027 (2012).
[29] A. Tyra, J. Li, Y. Shang, S. Jiang, Y. Zhao, and S. Xu, Physica A **482**, 713 (2017).
[30] A. Frieze and M. Karoński, *Introduction to Random Graphs* (Cambridge University Press, Cambridge, 2016).
[31] M. Golosovsky and S. Solomon, Phys. Rev. E **95**, 012324 (2017).
[32] P. Sheridan and T. Onodera, Sci. Rep. **8**, 2811 (2018).
[33] P. Holgate, Commun. Stat. Theor. M. **18**, 4539 (1989).
[34] S. Li and S. Wen, Complexity **2017**, 9781890 (2017).
[35] R. Devooght, A. Mantrach, I. Kivimäki, H. Bersini, A. Jaimes, and M. Saerens, in *Proc. of the 23rd Int. World Wide Web Conf.* (ACM, Seoul, Korea, 2014), pp. 213–224.
[36] D. Zhou and A. Elmokashfi, PLoS ONE **12**, e0189624 (2017).